Crystal structure of Mdm12 and combinatorial reconstitution of Mdm12/Mmm1 ERMES complexes for structural studies
A.P. AhYoung *et al.*
Biochemical and Biophysical Research Communications **488**, 129-135 *(2017)* **http://dx.doi.org/10.1016/j.bbrc.2017.05.021**

Appendix A. Supplementary data

Table S1. Diffraction data collection and structure refinement statistics

Protein	***Sce*-Mdm12 PDB ID 5VKZ**	**Mdm12/ Mmm1Δ**
Data set	**APS 042311 24-ID-C**	**ALS 101716 831**
Data collection statistics		
Wavelength	0.97918 Å	0.97918 Å
Resolution (last shell)	85.3-4.1 Å (4.21-4.10 Å)	20.13-4.50 Å (4.62-4.50 Å)
Unique reflections	10,272 (744)	7,867 (564)
Completeness	99.5 % (99.7 %)	98.3 % (99.8 %)
I/σ(I)	9.4 (2.0)	16.6 (1.6)
redundancy	7.4 (7.5)	3.9 (3.8)
R_{sym}	10.6 % (98.1 %)	3.1 % (93.5 %)
R_{meas} [a]	11.5 % (105.4 %)	3.6 % (108.9 %)
CC(1/2) [b]	99.8 % (95.8 %)	100.0 % (65.5 %)
Space group	$P3_221$	4/mmm (Laue class)
Unit cell dimensions	a=b=116.0 Å and c=161.7 Å	a=b=167.0 Å c=89.2 Å
AU content	2 molecules (pseudo-dimer)	1 complex
Solvent content	78 %	54 %
Refinement statistics		
Resolution	85.3-4.1 Å (4.58-4.10 Å)	-
Reflections	10,248	-
work set / test set	9,229 / 1,019	-
R_{free} / R_{cryst}	26.3 % / 24.8 %	-
Map correlation *Fo-Fc* (free)	82.8 % (88.0 %)	-
ESD Luzzati plot	1.383 Å	-
B_{wilson}	143 $Å^2$	-
$B_{average}$	162 $Å^2$	-
rmsd bonds	0.01 Å	-
rmsd angles	1.32 °	-
Ramachandran analysis		
allowed regions	88.9%	-
generously allowed	9.2%	-
outliers	1.4%	-

r.m.s.d. is the root-mean square deviation from ideal geometry.
$R_{sym} = \sum_{hkl}\sum_i |I_{hkl,i}-\langle I_{hkl,i}\rangle|/\sum_{hkl}\sum_i |I_{hkl,i}|$ where $\langle I_{hkl,i}\rangle$ is the average intensity of the multiple hkl, i observations for symmetry-related reflections.
R_{meas} is the redundancy independent R-factor [1].
CC(1/2) percentage of correlation between intensities from random half-datasets [2].
$R_{cryst} = \sum|F_{obs}-F_{calc}|/\sum|F_{obs}|$. F_{obs} and F_{calc} are observed and calculated structure factors, R_{free} is calculated from a set of randomly chosen reflections (10%), and R_{cryst} is calculated over the remaining reflections.
Structure quality was assessed in *MolProbity* [3] and *Polygon* [4].

Table S2. Small angle X-ray scattering analysis of the Mdm12/Mmm1Δ complex

protein	oligomeric state	calculated values from structures [a]		experimental values determined by SAXS [b] *Fourier analysis*	
		R_G	D_{max}	R_G	D_{max}
Mdm12	**monomer**	**21.9 Å**	**72 Å**	**-**	**-**
	dimer	**30.7 Å**	**108 Å**	**-**	**-**
complex	**hetero-tetramer**	**55.3 Å**	**195 ± 5 Å**	**46.7 ± 0.3 Å**	**185 ± 5 Å**

[a] the sets of theoretical R_G and D_{max} values correspond to the monomeric X-ray structure described in this study (PDB 5VKZ), the previously published Mdm12 dimeric structures (PDBs 5GYD and 5GYK) [5] and our pseudo-atomic model based on our NS-EM data of the Mdm12/Mmm1Δ complex [6], as shown in Figures 4A and 4B.

[b] experimental values of R_G and D_{max} were determined for the Mdm12/Mmm1Δ complex purified and crystallized as described in this work. Concentration of sample analyzed by SAXS ranged from 0.75 to 3 mg/ml and 4.8 to 14 mg/ml for the Guinier (low *q* range) and *P(r)* (high *q* range) analyses, respectively.

Crystal structure of Mdm12 and combinatorial reconstitution of Mdm12/Mmm1 ERMES complexes for structural studies
A.P. AhYoung *et al.*
Biochemical and Biophysical Research Communications **488**, 129-135 *(2017)* **http://dx.doi.org/10.1016/j.bbrc.2017.05.021**

pRSF His-MBP-Sce Mmm1Δ 31,219 Da

MGHHHHHHHHKIEEGKLVIWINGDKGYNGLAEVGKKFEKDTGIKVTVEHPDKLEEKFPQVAATGDGPDIIFWAHDRFGGYAQSGLL
AEITPDKAFQDKLYPFTWDAVRYNGKLIAYPIAVEALSLIYNKDLLPNPPKTWEEIPALDKELKAKGKSALMFNLQEPYFTWPLIA
ADGGYAFKYENGKYDIKDVGVDNAGAKAGLTFLVDLIKNKHMNADTDYSIAEAAFNKGETAMTINGPWAWSNIDTSKVNYGVTVLP
TFKGQPSKPFVGVLSAGINAASPNKELAKEFLENYLLTDEGLEAVNKDKPLGAVALKSYEEELAKDPRIAATMENAQKGEIMPNIP
QMSAFWYAVRTAVINAASGRQTVDEALKDAQTNSSSPGLVPRGSGKQHYELNEEAENEHLQELALILEKTYYNVDVHPAESLDWFN
VLVAQIIQQFRSEAWHRDNILHSLNDFIGRKSPDLPEYLDTIKITELDTGDDFPIFSNCRIQYSPNSGNKKLEAKIDIDLNDHLTL
GVETKLLLNYPKPGIAALPINLVVSIVRFQACLTVSLTNAEEFASTSNGSSSENGMEGNSGYFLMFSFSPEYRMEFEIKSLIGSRS
KLENIPKIGSVIEYQIKKWFVERCVEPRFQFVRLPSMWPRSKNTREEKPTELLVPRGSHHHHHHHHHH*

pCDF *Sce* Mdm12-His (C92S point mutation) 31,178 Da

MSFDINWSTLESDNRLNDLIRKHLNSYLQNTQLPSYVSNLRVLDFDLGKVGPAITLKEITDPLDEFYDSIREEADQETEENNDNKE
DSEHISPDRTIANHEGPKDDFEAPVVMPSPNDIQFLLEVEYKGDLLVTIGADLVLNYPVEKFMTLPVKLSISDIGLHSLCIVACLS
KQLFLSFLCDVSDPALDDNQTVLDPKGPILAATKPLERISIVRSMKIETEIGEQYQGQGSVLRSVGELEQFLFTIFKDFLRKELAW
PSWINLDFNDGDELVPRGSHHHHHH*

pCDF His-MBP-*Scas* Mdm12 27,709 Da

MGHHHHHHHHKIEEGKLVIWINGDKGYNGLAEVGKKFEKDTGIKVTVEHPDKLEEKFPQVAATGDGPDIIFWAHDRFGGYAQSGLL
AEITPDKAFQDKLYPFTWDAVRYNGKLIAYPIAVEALSLIYNKDLLPNPPKTWEEIPALDKELKAKGKSALMFNLQEPYFTWPLIA
ADGGYAFKYENGKYDIKDVGVDNAGAKAGLTFLVDLIKNKHMNADTDYSIAEAAFNKGETAMTINGPWAWSNIDTSKVNYGVTVLP
TFKGQPSKPFVGVLSAGINAASPNKELAKEFLENYLLTDEGLEAVNKDKPLGAVALKSYEEELAKDPRIAATMENAQKGEIMPNIP
QMSAFWYAVRTAVINAASGRQTVDEALKDAQTNSSSPGLVPRGSFNINWSEIGSDASISEAVKDHLSSYLQNVSLPSFVNNLKITD
FSFGAIAPTIILKEITDPLPDFYESVNEGLVEGDEGWTIPSPSDTQFLIEVEYKGDLFVTMSGELVLNYPSQEFIKLPIKLAVTNI
GFHSLCLVAYLAKQIFVSILCDVSDPILDEQNSEPLLDPNGTFMAPKKPFERISIIRSMNIDTEIGQQYQGEGSTLKNVGKLEQFL
LEKFKDLLRKEIAWPSWINLDLSGDNNELVPRGSHHHHHH*

pCDF His-MBP-*Ddis* Mdm12 23,171 Da

MGHHHHHHHHKIEEGKLVIWINGDKGYNGLAEVGKKFEKDTGIKVTVEHPDKLEEKFPQVAATGDGPDIIFWAHDRFGGYAQSGLL
AEITPDKAFQDKLYPFTWDAVRYNGKLIAYPIAVEALSLIYNKDLLPNPPKTWEEIPALDKELKAKGKSALMFNLQEPYFTWPLIA
ADGGYAFKYENGKYDIKDVGVDNAGAKAGLTFLVDLIKNKHMNADTDYSIAEAAFNKGETAMTINGPWAWSNIDTSKVNYGVTVLP
TFKGQPSKPFVGVLSAGINAASPNKELAKEFLENYLLTDEGLEAVNKDKPLGAVALKSYEEELAKDPRIAATMENAQKGEIMPNIP
QMSAFWYAVRTAVINAASGRQTVDEALKDAQTNSSSPGLVPRGSLKIYWDRVTEKHSIKLMNYLNERISGLTETYDMVGEMKITNL
SLGSKPPKFEIIQISDPDALILGNKSPNGIELRAKIGYDGDAYIGIQAEFKVNLPTPNFISFPVNVKVSNPIFSGIATVIYDTDKV
SFSFLPENGDSPDDFTPLKDVKFETQLGDSAQQVLVDLDKLQNFIVDLIKTYLKKYLVFPNKMTIPLSEFNNLVPRGSHHHHHH*

pJexp *Sce* Mdm12T4L-His 46,878 Da

MSFDINWSTLESDNRLNDLIRKHLNSYLQNTQLPSYVSNLRVLDFDLGKVGPAITLKEITDPLDEFYDSIREEADQETEENNDNKE
DSGSSGNIFEMLRIDEGLRLKIYKDTEGYYTIGIGHLLTKSPSLNAAKSELDKAIGRNTNGVITKDEAEKLFNQDVDAAVRGILRN
AKLKPVYDSLDAVRRAALINMVFQMGETGVAGFTNSLRMLQQKRWDEAAVNLAKSRWYNQTPNRAKRVITTFRTGTWDAYAAGSPN
DIQFLLEVEYKGDLLVTIGADLVLNYPVEKFMTLPVKLSISDIGLHSLCIVACLSKQLFLSFLCDVSDPALDDNQTVLDPKGPILA
ATKPLERISIVRSMKIETEIGEQYQGQGSVLRSVGELEQFLFTIFKDFLRKELAWPSWINLDFNDGDELVPRGSHHHHHHHHH*

Histidine tag
Maltose Binding Protein
Proteolytic cleavage site for thrombin.
Mdm12 or Mmm1 protein. Underlined residues were replaced with the T4L protein insertion in the internal *Sce*-Mdm12T4L chimeric construct.
T4 Lysozyme

Fig. S1. Protein constructs used for the reconstitution of the different Mdm12 and Mdm12/ Mmm1Δ complexes. The molecular weight of each ERMES protein obtained after proteolytic treatment with thrombin (no histidine tag and/or MBP left) is indicated.

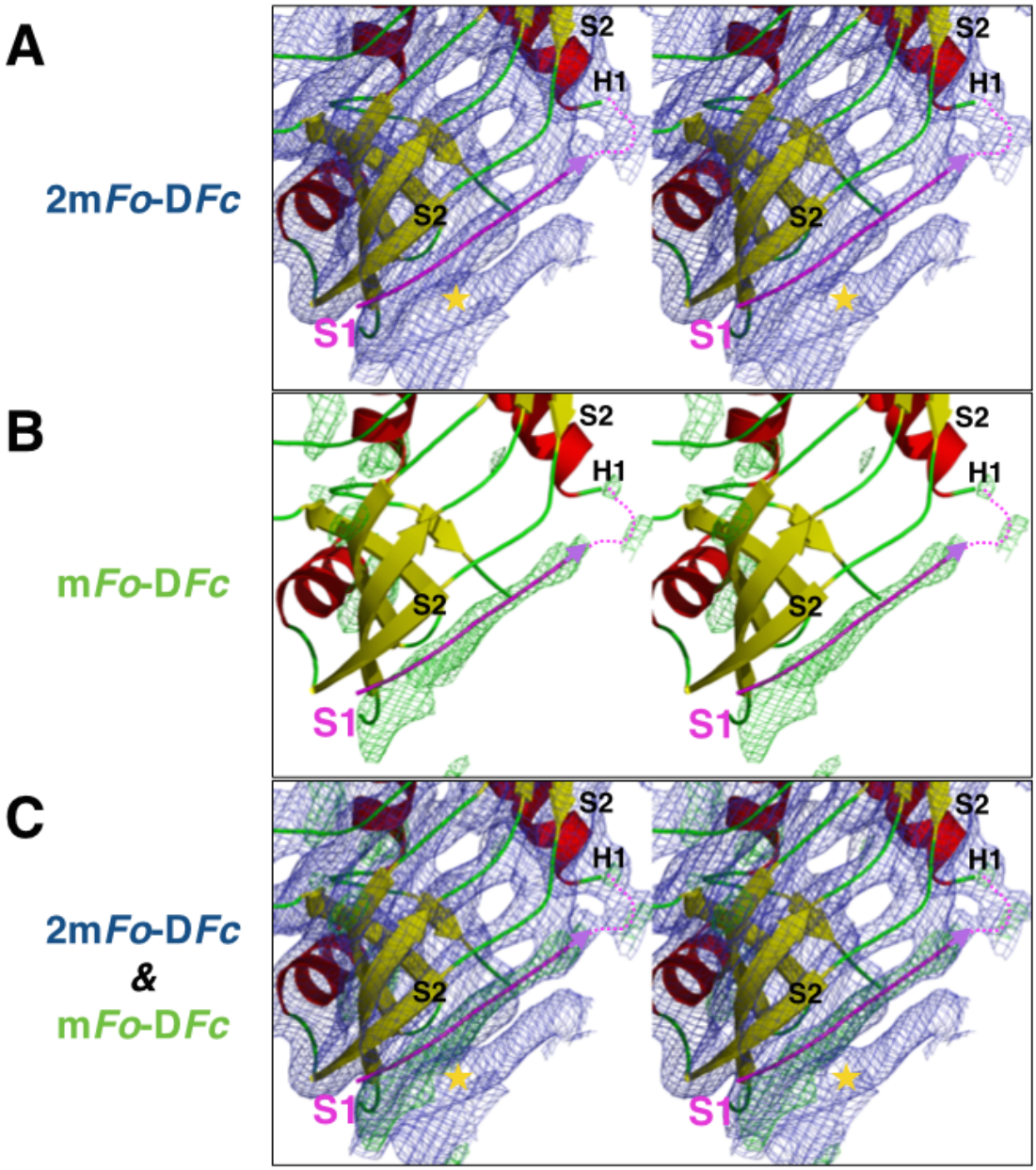

Fig. S2. **Unsharpened maximum likelihood weighted difference maps showing the non-swapped conformation of the N-terminal β-strand**. Stereo view of the initial 2m*Fo*-D*Fc* **(A)** and m*Fo*-D*Fc* **(B)** Fourier difference maps contoured at 1.1 σ and 3.0 σ, respectively, following molecular replacement in *Phaser* [7] and a single cycle of refinement in *Phenix* [8]. Molecular replacement was performed using the monomer of *Sce*-Mdm12 (PDB 5GYD) [5] as model where the 14 first N-terminal residues corresponding to the swapped β-strand S1 and the loop connecting with helix H1 were omitted. The backbone of Mdm12 is colored in red (helices), yellow (strands), and green (loops). The β-strand S1 drawn in magenta corresponds to the N-terminal β-strand S1 adopting a *non-swapped* conformation in our structure; it was *not* included in the initial model used for molecular replacement and the first cycle of refinement and is just shown to mark its true final position. (**C**) Same stereo view as in (**A**) and (**B**) but the two difference maps are shown superposed. These maps are *not* sharpened. The yellow star indicates a neighboring molecule (not displayed for clarity) related by crystallographic symmetry.

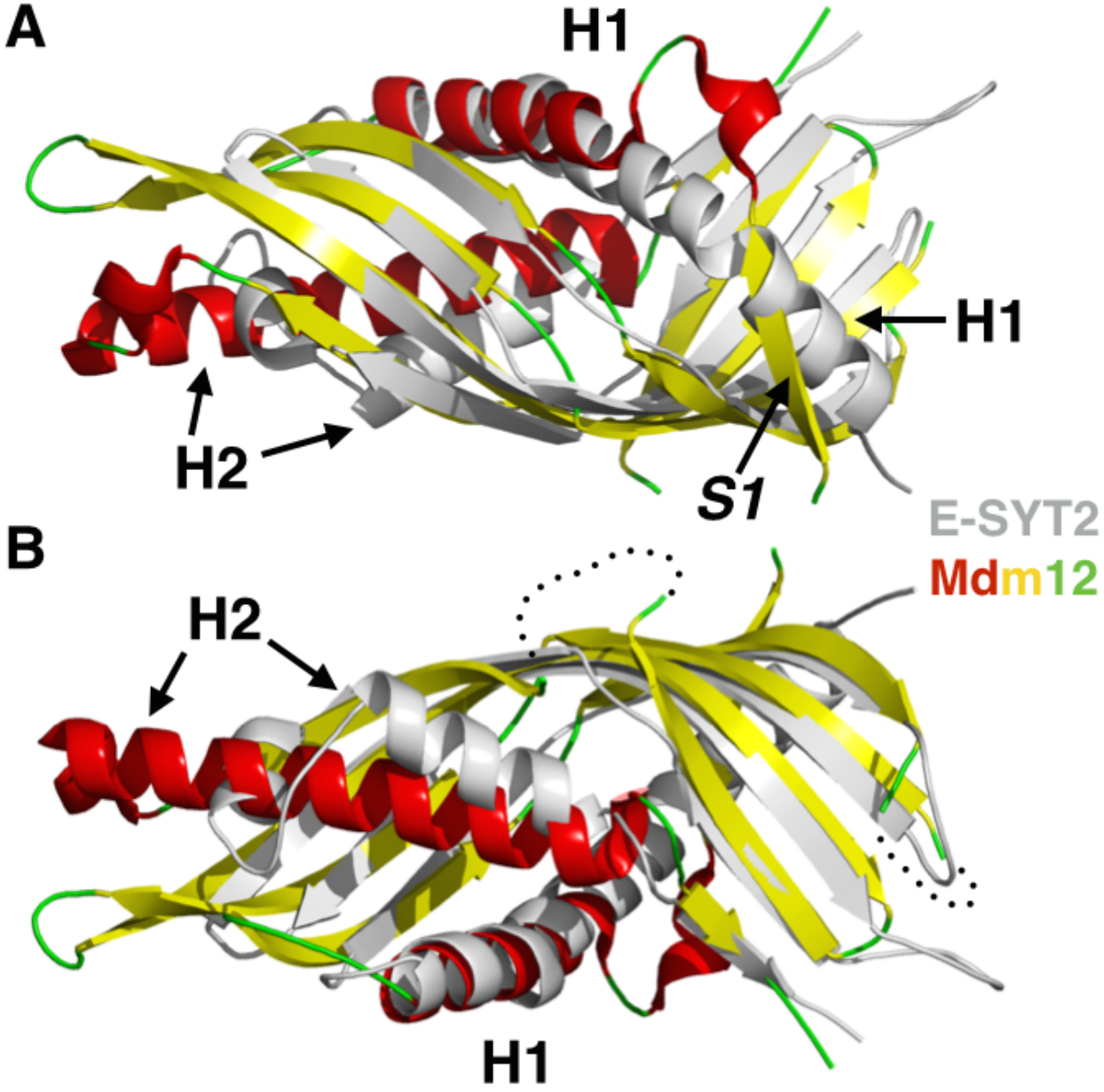

Fig. S3. **Superposition of the crystal structures of the SMP domains of Mdm12 and E-SYT2.** The superposed SMP folds observed in Mdm12 (yellow, green and red) and E-SYT2 (white) are shown in two different orientations (**A** and **B**) to highlight the most salient differences. For the sake of clarity, the two non-conserved insertions present in Mdm12 have been omitted and are shown as dotted lines. The two SMPs differ at their N-terminus with the presence of a N-terminal strand (S1) in Mdm12 replacing the bent N-terminus of the long α-helix H1 of E-SYT2. The other major difference is observed at the N-terminus of the α-helix H2; it is much shorter in the case of E-SYT2 [9]. The N-terminus of α-helix H1 of E-SYT2 is involved in its homo-dimerization, while the N-terminal β-strand S1 of Mdm12 that replaces it might play a similar role. In each SMP domain, the backbones of the antiparallel β-barrel formed by the 6 β-strands align remarkably well.

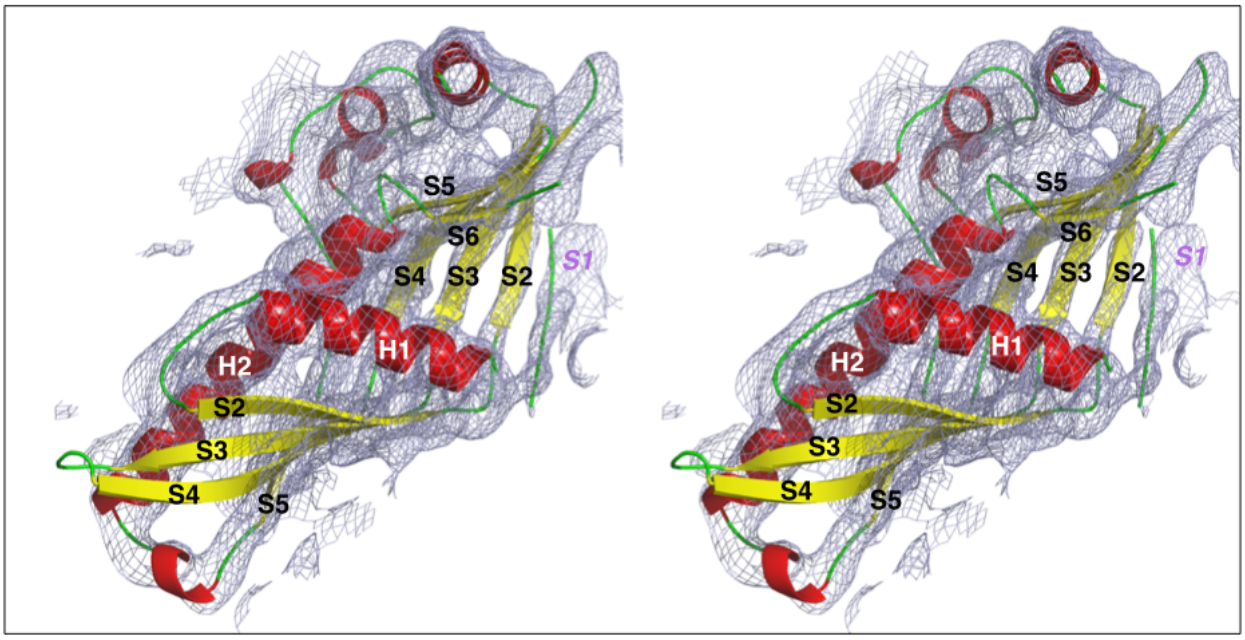

Fig. S4. Overall quality of the final maximum likelihood weighted 2m*Fo*-D*Fc* electron density for monomer A. Stereo-view of the unsharpened electron density map contoured at 1.3σ for the final refined structure shown in two different orientations. The non-swapped N-terminal β-strand S1 is highlighted in magenta. Secondary structure elements are labeled.

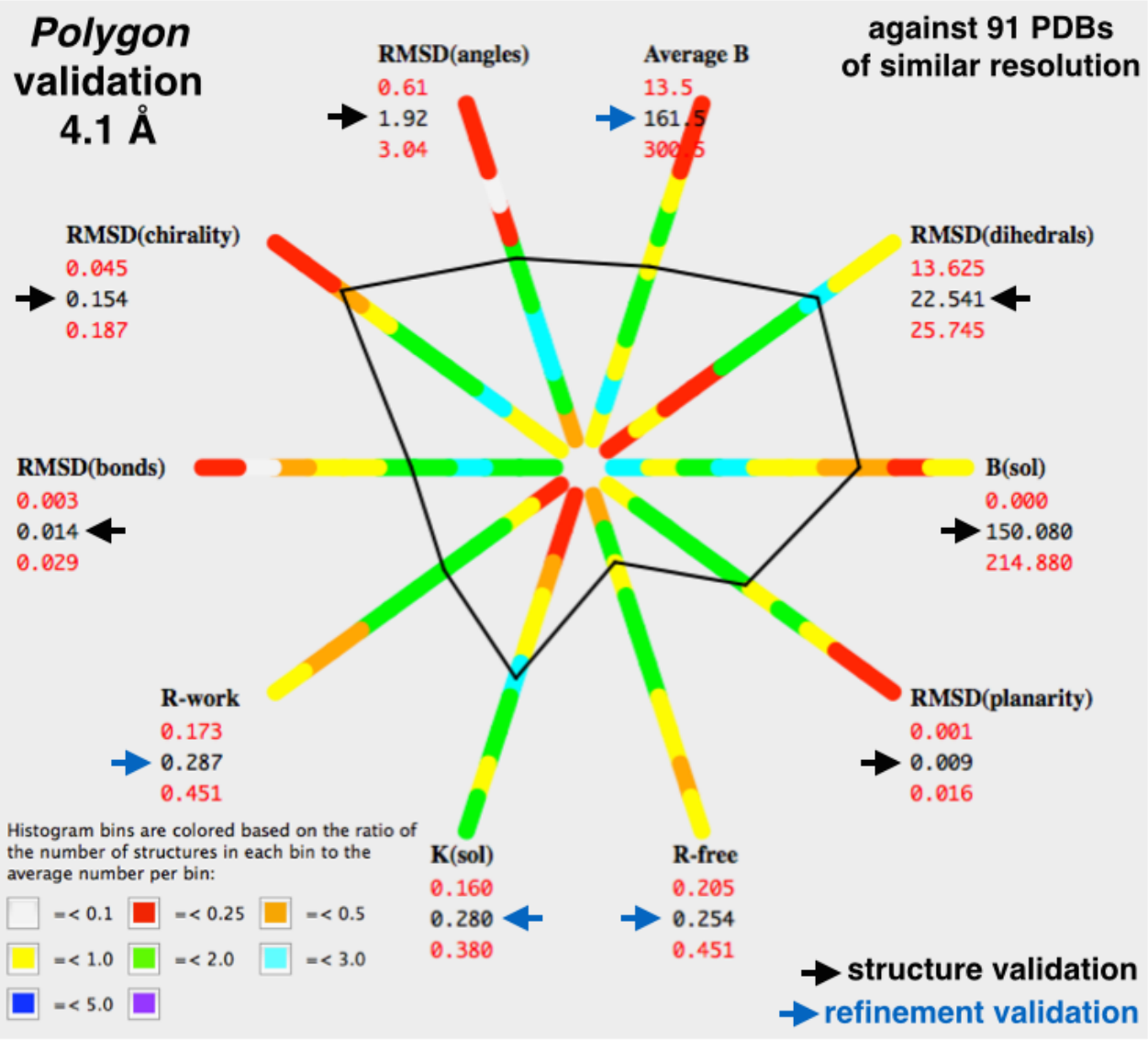

Fig. S5. **Structure and refinement quality assessment for the final model of *Sce*-Mdm12 refined at 4.1 Å resolution using *Polygon* analysis** [4]. The graph shows the histograms of the distribution across 91 PDB entries of similar resolution, with the range specified by numbers printed in red. Statistics for the current structure are printed in black (pointed by arrows); the connecting polygon (in black) shows where these values fall in the distribution.

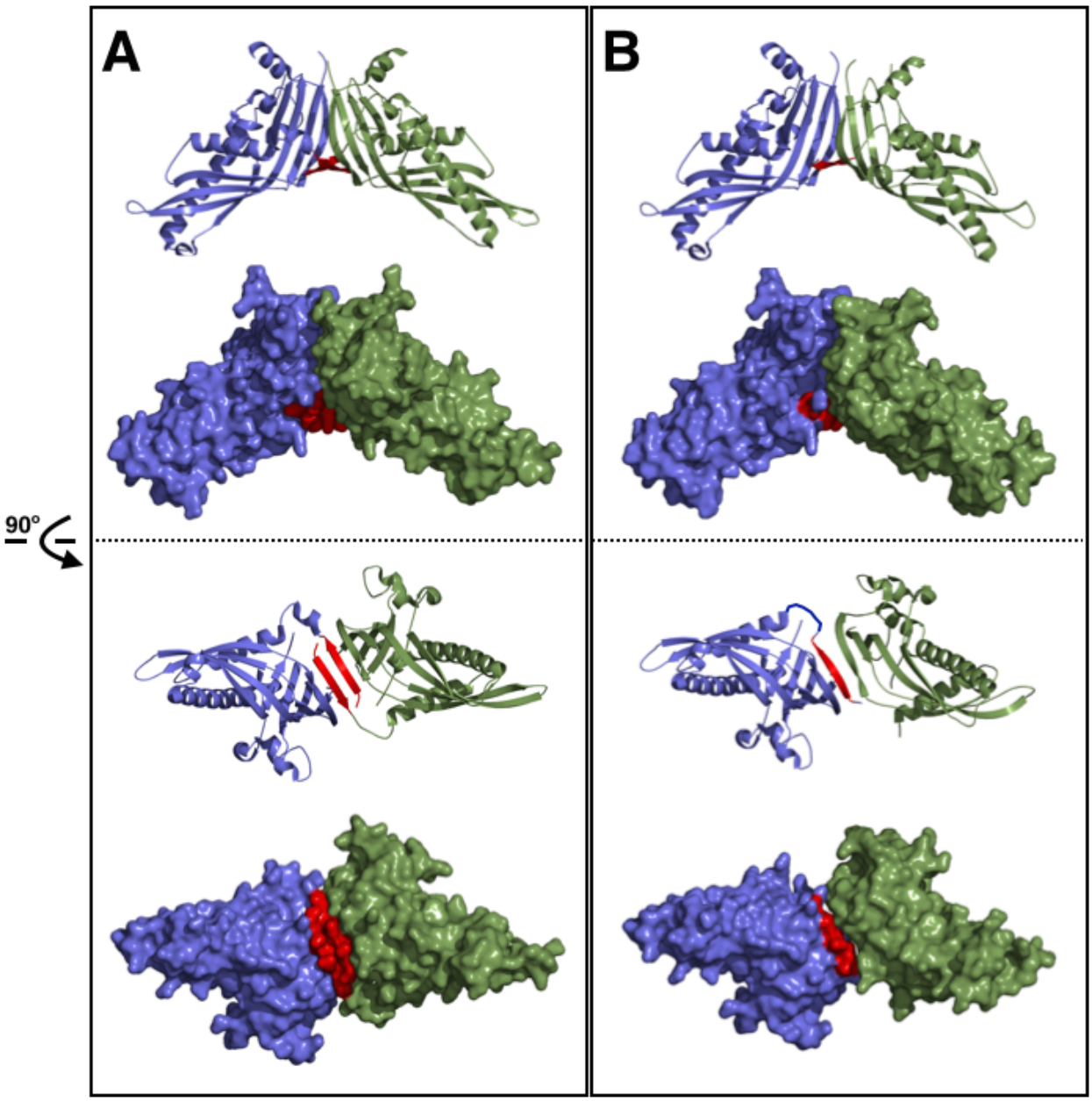

Fig. S6. The 'head-to-head' dimerization of the Mdm12 SMP/TULIP domain. Comparison between (**A**) the swapped 'head-to-head' dimer observed *in the asymmetric units* of structures 5GYD and 5GYK [5] and (**B**) our non-swapped 'head-to-head' pseudo-dimer observed *in the unit cell*. The N-terminal β-strand S1 is colored in red. Cartoon and surface representations are shown for two views (down the two-fold axis and perpendicular to the two-fold axis). Arrangement in (**A**) is the result of non-crystallographic symmetry while arrangement in (**B**) is a result of crystallographic symmetry.

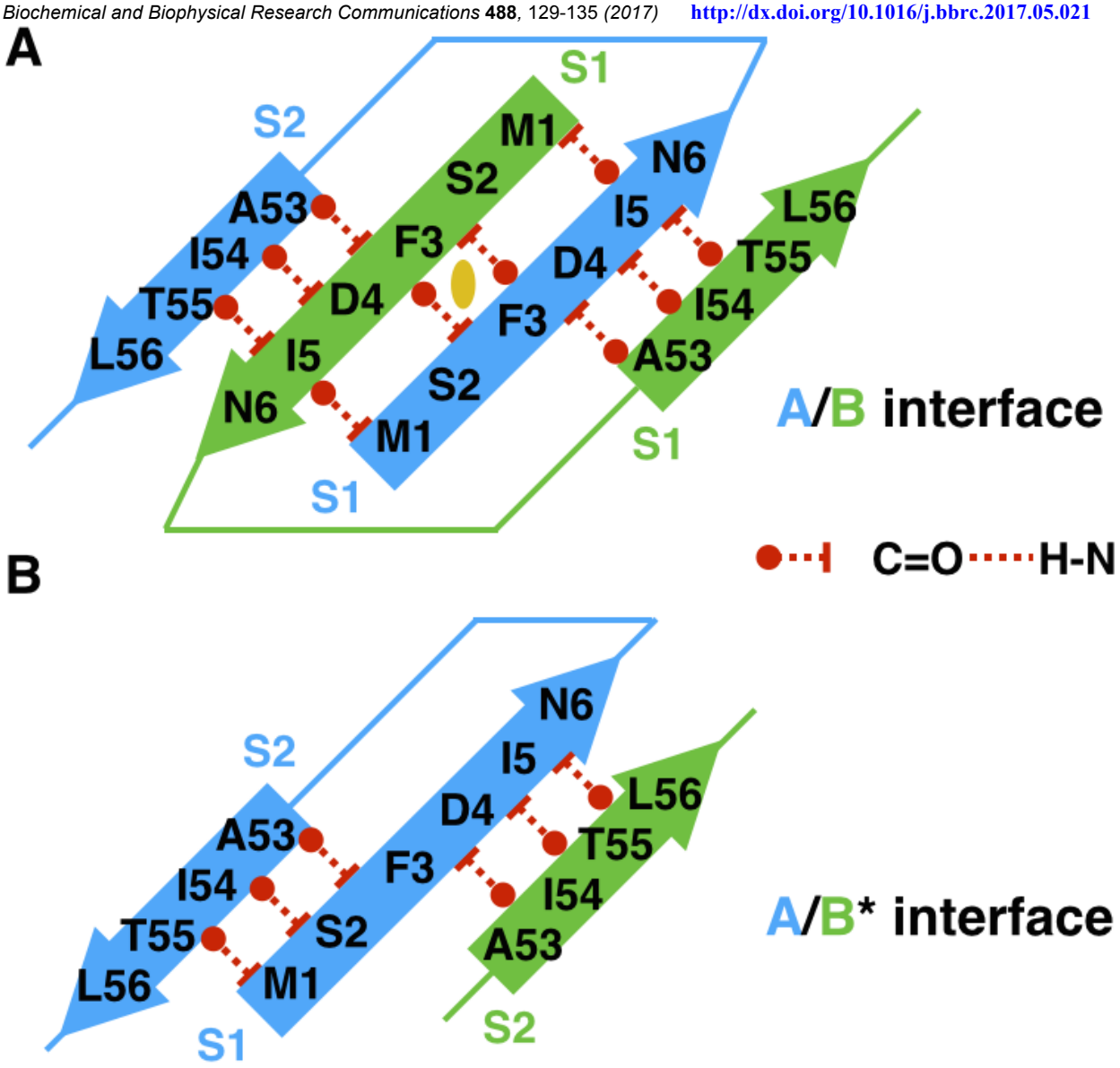

Fig. S7. Schematic of the interactions between the N-terminal β-strand S1 and the SMP/TULIP fold in Mdm12 (β-strand S2). (A) Swapping of N-terminal β-strands S1 at the two-fold symmetric 'head-to-head' dimerization interface described by Jeong *et al.* (PDBs 5GYD and 5GYK) [5]. **(B)** Asymmetric interface in the crystallographic 'head-to-head' pseudo-dimer interface observed in our structure.

References to Supplementary Data

[1] K. Diederichs, P.A. Karplus, Improved R-factors for diffraction data analysis in macromolecular crystallography, Nat Struct Biol 4 (1997) 269-275.
[2] P.A. Karplus, K. Diederichs, Linking crystallographic model and data quality, Science 336 (2012) 1030-1033.
[3] V.B. Chen, W.B. Arendall, 3rd, J.J. Headd, D.A. Keedy, R.M. Immormino, G.J. Kapral, L.W. Murray, J.S. Richardson, D.C. Richardson, MolProbity: all-atom structure validation for macromolecular crystallography, Acta Crystallogr D Biol Crystallogr 66 (2010) 12-21.
[4] L. Urzhumtseva, P.V. Afonine, P.D. Adams, A. Urzhumtsev, Crystallographic model quality at a glance, Acta Crystallographica Section D-Biological Crystallography 65 (2009) 297-300.
[5] H. Jeong, J. Park, C. Lee, Crystal structure of Mdm12 reveals the architecture and dynamic organization of the ERMES complex, EMBO Rep (2016).
[6] A.P. AhYoung, J. Jiang, J. Zhang, X. Khoi Dang, J.A. Loo, Z.H. Zhou, P.F. Egea, Conserved SMP domains of the ERMES complex bind phospholipids and mediate tether assembly, Proc Natl Acad Sci U S A 112 (2015) E3179-3188.
[7] A.J. McCoy, R.W. Grosse-Kunstleve, P.D. Adams, M.D. Winn, L.C. Storoni, R.J. Read, Phaser crystallographic software, J Appl Crystallogr 40 (2007) 658-674.
[8] P.D. Adams, P.V. Afonine, G. Bunkoczi, V.B. Chen, N. Echols, J.J. Headd, L.W. Hung, S. Jain, G.J. Kapral, R.W. Grosse Kunstleve, A.J. McCoy, N.W. Moriarty, R.D. Oeffner, R.J. Read, D.C. Richardson, J.S. Richardson, T.C. Terwilliger, P.H. Zwart, The Phenix software for automated determination of macromolecular structures, Methods 55 (2011) 94-106.
[9] C.M. Schauder, X. Wu, Y. Saheki, P. Narayanaswamy, F. Torta, M.R. Wenk, P. De Camilli, K.M. Reinisch, Structure of a lipid-bound extended synaptotagmin indicates a role in lipid transfer, Nature (2014).